Propagation of Squeezed Vacuum under Electromagnetically Induced Transparency

Eden Figueroa[1]‡**, Mirko Lobino**[1]**, Dmitry Korystov**[1]**, Jürgen Appel**[1]§ **and A. I. Lvovsky**[1]

[1] Institute for Quantum Information Science, University of Calgary, Calgary, Alberta T2N 1N4, Canada

Abstract. We analyze the transmission of continuous-wave and pulsed squeezed vacuum through rubidium vapor under the conditions of electromagnetically induced transparency. Our analysis is based on a full theoretical treatment for a squeezed state of light propagating through temporal and spectral filters and detected using time- and frequency-domain homodyne tomography. A model based on a three-level atom allows us to evaluate the linear losses and extra noise that degrade the nonclassical properties of the squeezed vacuum during the atomic interaction and eventually predict the quantum states of the transmitted light with a high precision.

PACS numbers: 42.50.Gy, 03.67.-a, 42.50.Dv

‡ Present address: Max-Planck-Institut für Quantenoptik, Hans-Kopferman-Strasse 1, D-85748 Garching, Germany.
§ Present address: Niels Bohr Institute Blegdamsvej 17 DK - 2100 København Denmark.

1. Introduction

Electromagnetically-induced transparency (EIT) was first introduced [1] as a technique to create a transparency window in an otherwise opaque medium. Years later, Fleischhauer and Lukin [2] suggested EIT as means for implementing quantum memory for light, i.e. transferring the state of the electromagnetic field to a collective atomic spin excitation. After the first proof-of-principle experimental realization of this protocol with classical light pulses [3], several experimental groups demonstrated that EIT-based memory can preserve nonclassical properties of light.

Such experiments became possible with the development of quantum light sources with wavelength and bandwidth characteristics enabling strong interaction with the atomic media. Two main approaches have been pursued. First, the Duan-Lukin-Cirac-Zoller procedure [4] has been used to generate narrowband photons which have then been stored and retrieved using the EIT method [5, 6]. Second, narrowband squeezed vacuum tuned to atomic transitions was created by sub-threshold optical parametric amplifiers (OPAs) [7, 8, 9], and used to prove the preservation of squeezing after slow propagation [10, 11, 12] and storage [13, 14]. This last method has also been used recently to preserve the continuous-variable entanglement in light slowed down by an EIT medium [15].

Also, various aspects of the EIT interaction for squeezed light have been analyzed [16]. Special attention has been paid to the excess quadrature noise generated by atoms illuminated by the EIT control field [17, 18], which was also studied experimentally [19].

However, none of the previous publications on slowdown and storage of continuous-variable optical states reported a satisfactory comparison of theoretical models with experimental data. In this paper we fill this void by presenting for the first time a full theoretical and experimental study of the transmission of squeezed light through an EIT medium both in the continuous-wave and pulsed regimes. Our theoretical model uses a series of spectral and time-domain measurements of the transmission of a classical field under EIT in order to fit the standard expression for the linear susceptibility of a 3-level atomic system. Subsequently we use the susceptibility to calculate the effect of propagation through an EIT medium of the squeezed vacuum generated by our OPA, both in the continuous-wave(CW) and pulsed cases. Then we perform two experimental tests: in the continuous regime, we measure the quadrature noise spectra of the transmitted squeezed vacuum and, in the pulsed regime, we perform complete quantum-state reconstruction via time-domain homodyne tomography. The analysis identifies all main sources of degradation of squeezing, enabling us to predict the experimental result with an over 99 % quantum-mechanical fidelity.

1.1. Experimental setup

The EIT medium was an atomic ^{87}Rb vapor at 65°C, with a Λ energy level configuration formed by one of the hyperfine sublevels of the $5P_{1/2}$ state and two hyperfine sublevels of the $5S_{1/2}$ state (Fig. 1, inset). The classical signal field, resonant to the $\left|5S_{1/2}, F = 1\right\rangle$–
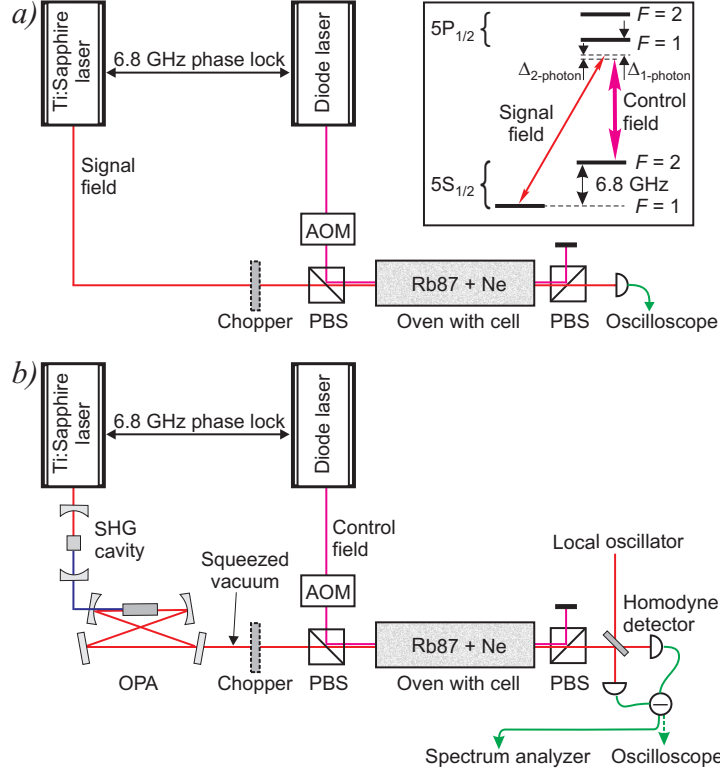
Figure 1. Experimental setup for classical (a) and quantum (b) measurements. SHG, second harmonic generation; PBS, polarizing beam splitter; AOM, acousto optical modulator. The elements used in experiments with pulsed light are shown with a dashed line. The inset displays the atomic energy level configuration.

$\left|5P_{1/2}, F = 1\right\rangle$ transition, was provided by a Ti:Sapphire laser at a wavelength of 795 nm [Fig. 1(a)]. The squeezed vacuum signal was obtained from a sub-threshold CW OPA with a bow-tie cavity, employing a 20-mm-long periodically poled $KTiOPO_4$ crystal as the nonlinear element [9]. The OPA was pumped by the second harmonic of the master Ti:Sapphire laser and generated a squeezing of approximately 3 dB. The same laser was used as the local oscillator in homodyne detection [Fig. 1(b)]. When required, the signal was chopped into 600-ns (FWHM) pulses using a home-made mechanical chopper [14]. The control field, interacting with the $\left|5S_{1/2}, F = 2\right\rangle$–$\left|5P_{1/2}, F = 1\right\rangle$ transition, was obtained from an additional diode laser phase locked at 6.834 GHz to the master laser to ensure a two-photon resonance with the signal. Orthogonal, linear polarizations for the control and signal were utilized. The two fields were focused to a diameter of about 130 μm and spatially mode matched inside the Rb cell.

2. Classical measurements

The transmission of coherent light through rubidium atoms in the presence of a control field was measured in order to characterize the absorption and dispersion of the medium.
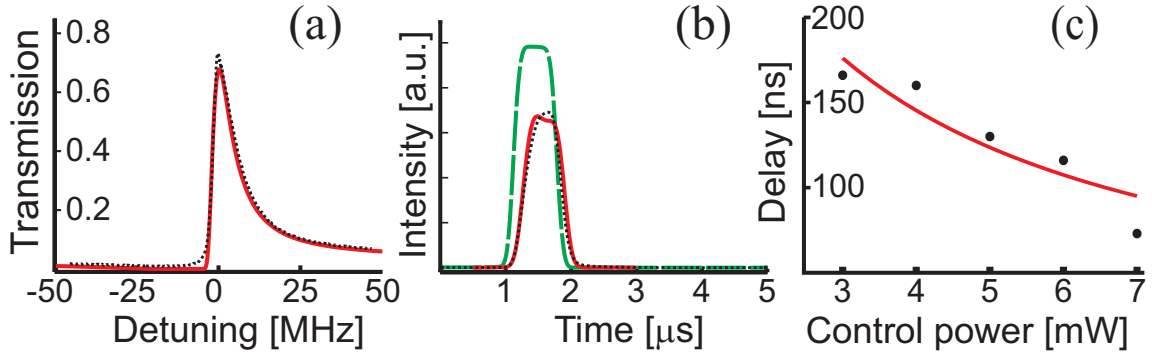
Figure 2. Transmission of classical light through the EIT medium. a) The EIT line transmission spectrum (dotted line) with a theoretical fit (solid line). The zero frequency corresponds to the two-photon resonance between the signal and control fields. b) Classical input pulse (dashed line), the slowed down pulse (dotted line), and a theoretical fit (solid line). c) Time delays for different control powers The size of the dot represents the margin of error ($\pm$ 2 ns). In (a) and (b), results for 5-mW control field power are displayed.

Assuming a 3-level system, these properties are governed by the linear susceptibility

$$\chi(\Delta_p, \delta_2) \propto \frac{i\gamma_{bc} + \delta_2}{|\Omega|^2 - (i\gamma_{bc} + \delta_2)(\Delta_p + iW)} \tag{1}$$

of a Doppler broadened gas under EIT conditions [20]. In the above equation, Ω is the control Rabi frequency, Δ_p is the one-photon detuning of the signal field, δ_2 is the two-photon detuning, γ_{bc} is the ground state dephasing rate, and W is the width of the Doppler-broadened line. The susceptibility determines the transmitted amplitude of the different frequency components of the input field $E_{in}(\omega)$ through the atomic ensemble by:

$$E_{out}(\omega) = e^{i\frac{\omega}{2c}\chi L} E_{in}(\omega), \tag{2}$$

where L is the medium length, ω is the angular frequency and amplitude transmissivity is given by $T(\omega) = e^{i\frac{\omega}{2c}\chi L}$. The inverse Fourier transform of Eq. (2) is used in deriving the temporal profile of the transmitted pulse as shown in Fig 2(b) while the time delay was calculated using the center of mass of the intensity profile.

Equation (1) assumes pure dephasing (decay of the off-diagonal element of the density matrix) to be the main mechanism of the ground state decoherence. An alternative decoherence process, exchange of population between the two ground states, does not significantly affect the EIT transmission spectrum, as evidenced by our group's earlier investigations [20] and the quantum noise measurements described below.

The parameters in Eq. (1) were determined from the following two measurements, each performed with EIT control powers between 3 and 7 mW. First, the intensity transmission spectrum of the EIT window was determined by scanning the frequency of the control field laser while keeping the power and frequency of the signal beam constant [Fig. 2(a)]. Second, transmission of 600-ns signal pulses was measured in the

time domain, revealing information about the dispersion of the medium [Fig. 2(b)]. As expected from an EIT system, significant (up to a factor of a thousand) reduction of the group velocity of light has been observed [Fig. 2(c)].

The results were fitted with Eq. (1). The data for different control powers were fitted with the same set of parameters, except the control Rabi frequency, which was proportional to the square root of the control field intensity. Although treating the rubidium atom as a three-level system is an oversimplification, it turns out sufficient to obtain good agreement, as evidenced by Fig. 2.

3. Measurements on squeezed vacuum

3.1. Squeezed vacuum: CW measurements

3.1.1. OPA squeezing In order to predict the evolution of squeezing under EIT conditions, we need to revisit the classic theory of squeezing inside an OPA cavity as developed by Gardiner and Savage [21] and reviewed, for example, in Ref. [22].

In a degenerate, continuous-wave OPA pumped below threshold at frequency 2Ω, parametric-down conversion produces pairs of photons at lower frequency $\Omega \pm \omega$. In the Heisenberg picture, it can be described as nonlinear mixing of input vacuum fields $a_{\text{in}}(\pm\omega)$ associated with optical frequencies $\Omega \pm \omega$ (Bogoliubov transformation):

$$\hat{a}(\omega) = C(\omega)\hat{a}_{\text{in}}(\omega) + S(\omega)\hat{a}_{\text{in}}^\dagger(-\omega), \tag{3}$$

where, under certain approximations,

$$C(\omega) = 1 - 2\gamma\frac{\gamma - i\omega}{(\gamma - i\omega)^2 - \gamma^2 P/P_{th}}; \tag{4}$$

$$S(\omega) = 2\gamma^2\frac{\sqrt{P/P_{th}}}{(\gamma - i\omega)^2 - \gamma^2 P/P_{th}}.$$

In Eq. (4), P/P_{th} is the ratio of the OPA pump and threshold powers, and 2γ is the cavity bandwidth. Using $[a_{\text{in}}(\omega), a_{\text{in}}^\dagger(\omega')] = \delta(\omega - \omega')$, we find the correlations of the OPA output fields at different frequencies:

$$\langle\hat{a}^\dagger(\omega)\hat{a}(\omega')\rangle = S^*(\omega)S(\omega')\delta(\omega - \omega');$$
$$\langle\hat{a}(\omega)\hat{a}(\omega')\rangle = C(\omega)S(\omega')\delta(\omega + \omega'). \tag{5}$$

The frequency-domain quadrature observable associated with phase ϑ is defined as [23]

$$\hat{q}_\vartheta(\omega) = \frac{1}{\sqrt{2}}\left[\hat{a}(\omega)e^{i\vartheta} + \hat{a}^\dagger(-\omega)e^{-i\vartheta}\right]. \tag{6}$$

The phase-dependent quadrature noise is then given by

$$\begin{aligned}
\langle\hat{q}_\vartheta(\omega)\hat{q}_\vartheta(-\omega')\rangle = \frac{1}{2}\langle\hat{a}(\omega)\hat{a}^\dagger(\omega') &+ \hat{a}^\dagger(-\omega)\hat{a}(-\omega') \\
&+ \hat{a}(\omega)\hat{a}(-\omega')e^{+2i\vartheta} + \hat{a}^\dagger(-\omega)\hat{a}^\dagger(\omega')e^{-2i\vartheta}\rangle \\
&\equiv V_\vartheta(\omega)\delta(\omega - \omega'), \tag{7}
\end{aligned}$$

where

$$V_\vartheta(\omega) = \frac{1}{2}[1 + S^*(\omega)S(\omega) + S^*(-\omega)S(-\omega) \qquad (8)$$
$$+ \, C(\omega)S(-\omega)e^{+2i\vartheta} + C^*(\omega)S^*(-\omega)e^{+2i\vartheta}].$$

Analyzing Eq. (4), we find that $S^*(\omega) = S(-\omega)$ and $C(\omega)S(-\omega)$ is a real number for all frequencies, which allows the above expression to be simplified:

$$V_\vartheta(\omega) = \frac{1}{2} + |S(\omega)|^2 + C(\omega)S(-\omega)\cos(2\vartheta). \qquad (9)$$

In order to relate this quantity to the noise spectrum measured experimentally by means of homodyne detection, we need to account for imperfect quantum efficiency of the photodiodes and the optical losses inside and outside the OPA cavity. Equation (9) then becomes

$$V_\vartheta^{\text{exp}}(\omega) = \frac{1}{2} + \eta[|S(\omega)|^2 + C(\omega)S(-\omega)\cos(2\vartheta)], \qquad (10)$$

where η is the overall quantum efficiency. Substituting Eq. (4), we obtain the well-known result for the quadrature noise levels associated with phases $\vartheta = \pi/2$ (antisqueezed) and $\vartheta = 0$ (squeezed):

$$V^\pm(\omega) = \frac{1}{2} \pm \eta \frac{2\sqrt{P/P_{th}}}{(\omega/\gamma)^2 + (1 \mp \sqrt{P/P_{th}})^2}. \qquad (11)$$

Experimentally, we observe continuous-wave squeezing in the frequency domain by feeding the homodyne detector output to a spectrum analyzer. At each frequency, the local oscillator phase was varied and the highest and lowest noise levels were recorded. Figure 3(a) shows the experimentally measured highest and lowest quadrature noise levels of the OPA output and a theoretical fit with Eq. (11).

3.1.2. Propagation through the EIT medium We have placed the atomic vapor cell between the OPA and the homodyne detector and performed the frequency-domain measurement of the quadrature noise of the transmitted squeezed vacuum. We found that the squeezing is preserved better when the lasers are slightly detuned from the two-photon resonance. This is because the noise reduction observed at a specific electronic frequency ω originates from quadrature entanglement between the spectral modes associated with the frequencies $\Omega \pm \omega$ of the optical signal field. Thus both modes need to be transmitted through the EIT transparency window. Because our EIT lines are substantially asymmetric [Fig. 2(a)], one of the modes is strongly absorbed under the conditions of two-photon resonance. Figure 3(b) displays CW squeezing that remains after the interaction with rubidium atoms with a two-photon detuning of 540 kHz.

In our theoretical analysis, we assume two main degradation mechanisms. First, there is linear loss due to a finite width and imperfect transmission of the EIT line. Upon propagation through a medium with amplitude transmissivity $T(\omega)$, the field operator becomes $\hat{a}'(\omega) = \sqrt{\eta}T(\omega)\hat{a}(\omega) + \sqrt{1 - \eta|T(\omega)|^2}\hat{v}(\omega)$, where $\hat{v}(\omega)$ denotes vacuum. In

writing this equation we have assumed that the losses associated with the quantum efficiency η occur before the rubidium cell; assuming otherwise would not change the results below since only linear losses are involved. Substituting the new field operator into Eq. (7) and noticing that $\hat{a}(\omega)$ and $\hat{v}(\omega)$ are uncorrelated, we find for the quadrature noise

$$V'_\vartheta(\omega) = \frac{1}{2} + \frac{\eta}{2}[|S(\omega)|^2[|T(\omega)|^2 + |T(-\omega)|^2] \tag{12}$$
$$+ C(\omega)S(-\omega)[T(\omega)T(-\omega)e^{2i\vartheta} + T^*(\omega)T^*(-\omega)e^{-2i\vartheta}]].$$

From Eq. (10) we obtain

$$\eta|S(\omega)|^2 \quad = \frac{V^+(\omega) + V^-(\omega) - 1}{2}; \tag{13}$$
$$\eta C(\omega)S(-\omega) = \frac{V^+(\omega) - V^-(\omega)}{2},$$

which allows us to relate the maximum and minimum quadrature noise levels in the presence and absence of the vapor cell:

$$V'^\pm(\omega) = \frac{1}{2} + \frac{1}{2}\left[V^+(\omega) + V^-(\omega) - 1\right]\left[|T(\omega)|^2 + |T(-\omega)|^2\right] \tag{14}$$
$$\pm \left[V^+(\omega) - V^-(\omega)\right]|T(\omega)||T(-\omega)|.$$

Interestingly, for each detection frequency this noise depends only on the magnitude of $T(\omega)$, but not on the phase shift introduced by the rubidium gas. This is because any complex phase in the quantity $T(\omega)T(-\omega)$ in Eq. (12) that may be present due to asymmetric dispersion of the EIT line can be compensated by adjusting the local oscillator phase ϑ.

The degradation of squeezing in transmission through EIT occurs not only due to absorption but also because of extra noise $V_{\text{noise}}(\omega)$ generated by atoms in the cell [19]. This contribution is a consequence of the population exchange of the rubidium ground states and has been investigated theoretically in Refs. [17, 18]. We evaluated this noise independently by performing homodyne detection of the field emanated by the EIT cell in the absence of the input squeezed vacuum. The result of this measurement, with the shot noise subtracted, is shown in the inset of Fig. 3, along with a theoretical fit according to Ref. [18]. The only additional fitting parameter here is the population exchange rate, which determines the overall magnitude of the extra noise [24]. We estimate this rate to account for less than 10 % of all decoherence processes, which justifies our earlier assumption.

We account for the extra noise by adding $V_{\text{noise}}(\omega)$ to the right-hand side of Eq. (14). In this way, we construct a theoretical prediction for the spectrum of the transmitted squeezed vacuum. No additional fitting parameters are required. The agreement between theory and experiment in Fig. 3(b) shows that, indeed, absorption and the extra noise are the main factors responsible for the degradation of squeezing.
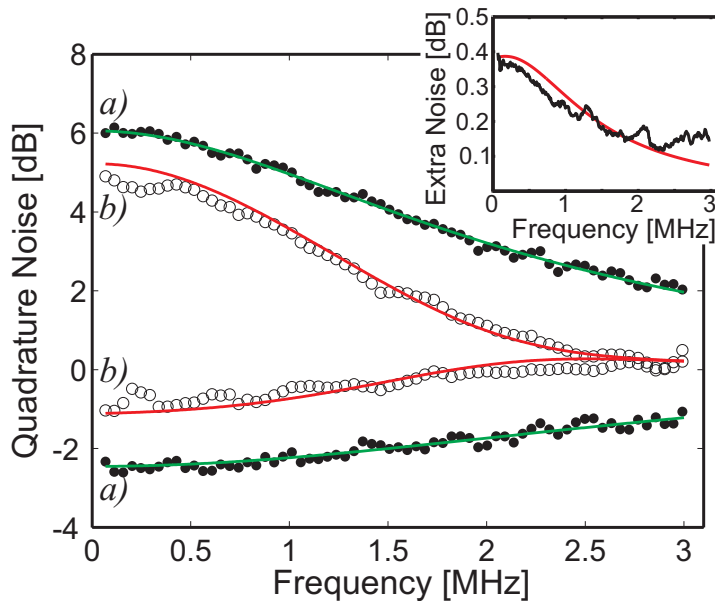
Figure 3. Squeezed and antisqueezed quadrature noise from the OPA (a) and after the EIT medium (b), along with the theoretical prediction of Eq. (11) and Eq. (14) plus the extra noise. Inset: atomic extra noise measured in the absence of the signal field. The control field power is 5 mW. The error bar is ± 0.05 dB and is smaller then the size of the dots.

3.2. Squeezed vacuum: pulsed measurements

We studied propagation of pulses of squeezed vacuum through the EIT medium by means of time-domain homodyne tomography, using a procedure similar to that of Ref. [25]. The output of the homodyne detector was multiplied by the temporal mode function $W(t)$ and integrated over time, producing a single sample of the field quadrature. The weight function was equal to the square root of the transmitted classical pulse intensity [dotted line in Fig. 2(b)]. In this manner, 50,000 quadrature samples were obtained. The local oscillator phase values associated with each quadrature were determined using the method described in Ref. [14], by measuring the degree of squeezing in the transmitted light with a spectrum analyzer running continuously. These data were used to reconstruct the density matrix and the Wigner function of the transmitted, pulsed optical mode by means of the maximum-likelihood algorithm[26] (Fig. 4). The reconstructed optical state strongly resembles a squeezed thermal state. The minimum and maximum noise levels observed at different control field powers are summarized in Fig. 5.

The experimental data on classical transmission of the EIT line, the parameters of the OPA and the atomic extra noise spectra are sufficient to make theoretical predictions for the transmission of squeezed vacuum in the pulsed regime without additional fitting parameters.

We now begin the analysis in the time domain. Suppose the output of the OPA

cavity is expressed by a time-dependent annihilation operator

$$\hat{a}(t) = \frac{1}{\sqrt{2\pi}} \int\limits_{-\infty}^{+\infty} \hat{a}(\omega)e^{-i\omega t}\mathrm{d}\omega. \tag{15}$$

After the chopper, this operator will change into $\hat{a}'(t) = \sqrt{\eta}\tau(t)\hat{a}(t) + \text{v.c.}$ with $\tau(t)$ representing the time-dependent transmission of the chopper and v.c. denoting the vacuum contribution whose explicit form will be calculated later. In order to account for the propagation through the cell, we switch to the frequency domain, replacing multiplication by convolution:

$$\hat{a}'(\omega) = \sqrt{\frac{\eta}{2\pi}} \int\limits_{-\infty}^{+\infty} \tilde{\tau}(\omega - \omega')\hat{a}(\omega')\mathrm{d}\omega' + \text{v.c.}, \tag{16}$$

where $\tilde{\tau}(\omega)$ is the Fourier images of the $\tau(t)$. Absorption in the rubidium cell is then described by

$$\hat{a}''(\omega) = T(\omega)\hat{a}'(\omega) + \text{v.c.} \tag{17}$$
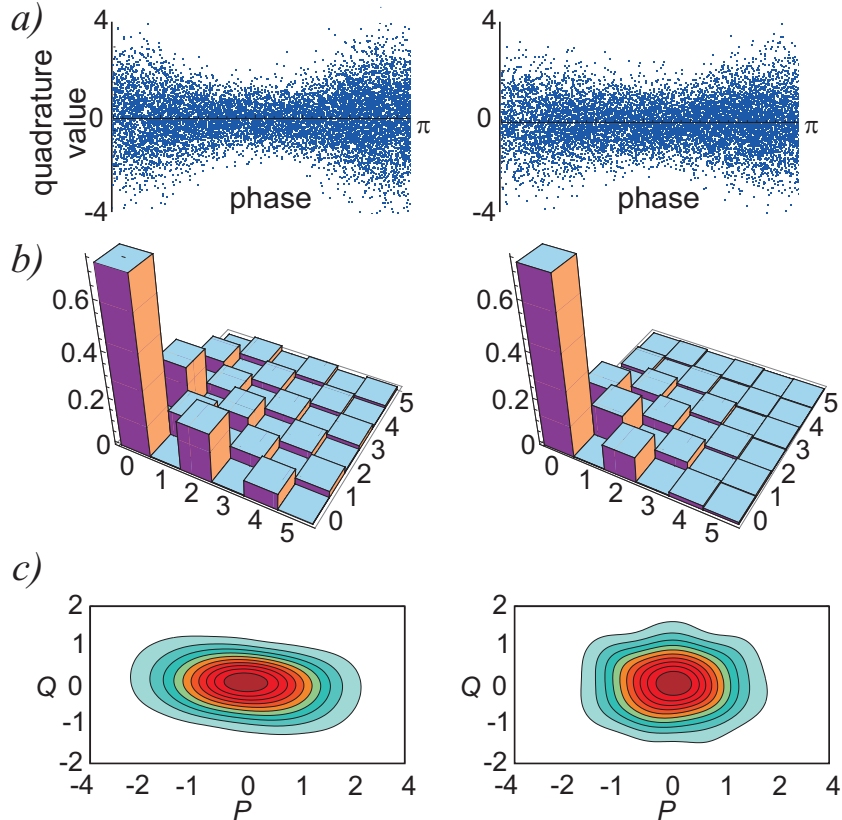
Figure 4. Quantum state of the input (left column) and slowed down (right column) squeezed vacuum with an EIT control power of 5 mW. Raw samples of phase-dependent quadrature noise (a), maximum-likelihood reconstruction of the density matrices in the Fock basis (absolute values, b) and Wigner functions (c) are shown.

After the cell, the quantum state of the temporal mode defined by the function $W(t)$ is subjected to homodyne tomography. The field operator associated with this mode is given by

$$\hat{A} = \int\limits_{-\infty}^{+\infty} \hat{a}''(t)W(t)\mathrm{d}t = \int\limits_{-\infty}^{+\infty} \hat{a}''(\omega)W(-\omega)\mathrm{d}\omega \qquad (18)$$

$$= \int\limits_{-\infty}^{+\infty} F(\omega)\hat{a}(\omega)\mathrm{d}\omega + \int\limits_{-\infty}^{+\infty} G(\omega)\hat{v}(\omega)\mathrm{d}\omega,$$

where

$$F(\omega) = \sqrt{\frac{\eta}{2\pi}} \int\limits_{-\infty}^{+\infty} T(\omega')W(-\omega')\tau(\omega' - \omega)\mathrm{d}\omega', \qquad (19)$$

$\hat{v}(\omega)$ is the vacuum field operator and the weight of the vacuum fraction is given by $G(\omega) = \sqrt{1 - |F(\omega)|^2}$. The measured (time-integrated) quadrature is given by $\hat{Q} = (\hat{A}e^{i\vartheta} + \hat{A}^\dagger e^{-i\vartheta})/\sqrt{2}$ and its variance, according to Eqs. (5) and (18) is

$$V''_\vartheta = \langle \hat{Q}^2 \rangle = \frac{1}{2} + V_{\mathrm{noise}} + \int\limits_{-\infty}^{+\infty} |F(\omega)|^2 |S(\omega)|^2 \qquad (20)$$

$$+ \frac{1}{2} \left[\int\limits_{-\infty}^{+\infty} C(\omega)S(-\omega)F(\omega)F(-\omega)e^{2i\vartheta} + \mathrm{c.c.} \right],$$

which using Eq. (13) simplifies to

$$V''_\vartheta = \frac{1}{2} + V_{\mathrm{noise}} + \frac{1}{2} \int_{-\infty}^{+\infty} |F(\omega)|^2 \left[V^+(\omega) + V^-(\omega) - 1 \right] d\omega \qquad (21)$$

$$+ \frac{1}{2} \int_{-\infty}^{+\infty} |F(\omega)F(-\omega)| \left[V^+(\omega) - V^-(\omega) \right] \cos(2\vartheta + \varphi(\omega)) d\omega$$

with $\varphi(\omega) = \arg[F(\omega)F(-\omega)]$. The pulsed atomic extra noise is obtained from the frequency-domain extra noise by integrating

$$V_{\mathrm{noise}} = \int_{-\infty}^{+\infty} |W(\omega)|^2 V_{\mathrm{noise}}(\omega) d\omega. \qquad (22)$$

Unlike the CW case, the phase shift imposed by the EIT line does lead to additional loss of squeezing. Because the EIT line is asymmetric [i.e. $T(-\omega) \neq T^*(\omega)$] and $\varphi(\omega)$ is not constant, the squeezed and antisqueezed quadratures may mix with each other in the integral (21).

The solid line in Fig. 5 shows the result of the calculation. For all control powers, over 99% fidelity (defined as $F = \mathrm{Tr}[(\hat{\rho}_{th}^{1/2}\hat{\rho}_{meas}\hat{\rho}_{th}^{1/2})^{1/2}]^2)$ between the theoretically predicted and experimentally observed states is reached.
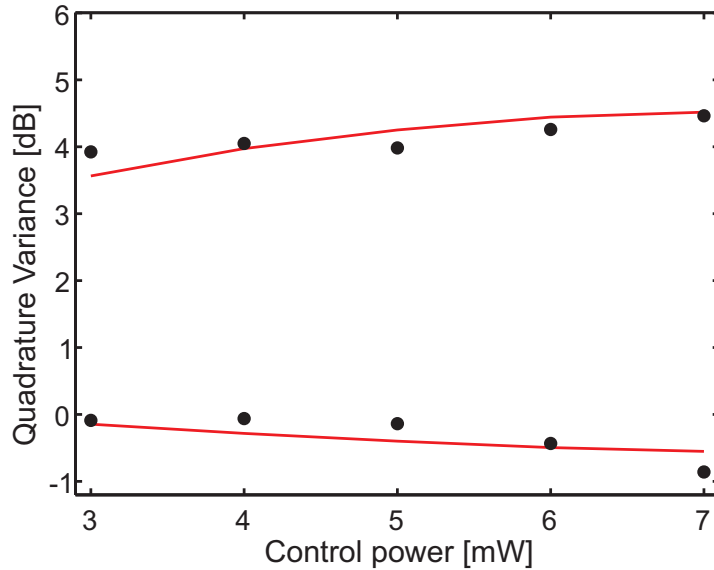
Figure 5. Maximum and minimum quadrature noise of pulsed squeezed vacuum transmitted through the EIT cell (theory and experiment). The size of the dot represents the margin of error ($\pm$ 0.05 dB).

4. Summary

We have performed a theoretical and experimental investigation of squeezed light propagation through an EIT medium in both the CW and pulsed regime. Starting with a theoretical expression for the susceptibility of the EIT medium, we determined the degradation of squeezing in each spectral component of the squeezed vacuum. For the pulsed case, we performed full quantum reconstruction of the optical state after propagation through the rubidium cell and compared it with the one predicted theoretically. We identified all main mechanisms leading to the degradation of squeezing: absorption in the EIT medium, asymmetry of the EIT line, and the extra noise induced by the control field. A very simple 3-level model is sufficient to fully explain our experimental results. This latter conclusion confirms a recent result of classical experiments on storage of light [27].

5. Acknowledgements

References

[1] Boller K J, Imamoglu A, Harris S E 1991 *Phys. Rev. Lett.* **66**, 2593

[2] Fleischhauer M and Lukin M D 2000 *Phys. Rev. Lett.* **84**, 5094; Fleischhauer M and Lukin M D 2002 *Phys. Rev. A* **65**, 022314

[3] Phillips D F, Fleischhauer A, Mair A, Walsworth R L, and Lukin M D 2001 *Phys. Rev. Lett.* **86**, 783

[4] Duan L M, Lukin M D, Cirac J I, and Zoller P 2001 *Nature* **414**, pp. 413-418

[5] Chanelière T, Matsukevich D, Jenkins S D, Lan S Y, Kennedy T A B and Kuzmich A 2006 *Nature* **438**, pp. 833-836

[6] Eisaman M D, André A, Massou F, Fleischhauer M, Zibrov A S and Lukin M D 2006 *Nature* **438**, 837

[7] Tanimura T, Akamatsu D, Yokoi Y, Furusawa A and Kozuma M 2007 *Opt. Lett.* **31**, 2344.

[8] Hetet G, Glöckl O, Pilypas K A, Harb C C, Buchler B C, Bachor H A and Lam PK 2007 *J. Phys. B: At. Mol. Opt. Phys.* **40** 221

[9] Appel J, Hoffman D, Figueroa E and Lvovsky A I 2007, *Phys. Rev. A* **75**, 035802

[10] Akamatsu D, Akiba K and Kozuma M 2004 *Phys. Rev. Lett.* **92**, 203602

[11] Akamatsu D, Yokoi Y, Arikawa M, Nagatsuka S, Tanimura T, Furusawa A and Kozuma M 2007 *Phys. Rev. Lett.* **99**, 153602

[12] Arikawa M, Honda K, Akamatsu D, Yokoil Y, Akiba K, Nagatsuka S, Furusawa A and Kozuma M 2007 *Opt. Express* **15**, 11849

[13] Honda K, Akamatsu D, Arikawa M, Yokoi Y, Akiba K, Nagatsuka S, Tanimura T, Furusawa A and Kozuma M 2008 *Phys. Rev. Lett.* **100**, 093601

[14] Appel J, Figueroa E, Korystov D, Lobino M and Lvovsky A I 2008 *Phys. Rev. Lett.* **100**, 093602

[15] Hétet G, Buchler B C, Glöckl O, Hsu M T L, Akulshin A M, Bachor H A and Lam P K 2008 *Opt Express* **16**, 7369

[16] Dantan A and Pinard M 2004 *Phys. Rev. A* **69**, 043810; Dantan A, Bramati A and Pinard M 2005 *Phys. Rev. A* **71** 043801; Dantan A, Cviklinski J, Pinard M and Grangier P 2006 *Phys. Rev. A* **73**, 032338

[17] Peng A, Johnsson M, Bowen W P, Lam P K, Bachor H A and Hope J J 2005 *Phys. Rev. A* **71**, 033809; Hétet G, Peng A, Johnsson M, Hsu M T L, Glöckl O, Lam P K, Bachor H A and Hope J J 2006 *Phys. Rev. A* **74**, 059902(E)

[18] Hétet G, Peng A, Johnsson M T, Hope J J and Lam P K 2008 *Phys. Rev. A* **77**, 012323

[19] Hsu M T L, Hétet G, Glöckl O, Longdell J J, Bucher B C, Bachor H A and Lam P K 2006 *Phys. Rev. Lett.* **97**, 183601

[20] Figueroa E, Vewinger F, Appel J and Lvovsky A I 2006 *Opt. Lett.* **31**, 2625

[21] Gardiner C W and Savage C M 1984 *Opt. Comm.* **50**, 173

[22] Scully M O and Zubairy M S 1997 *Quantum Optics* (Cambridge: Cambridge University Press)

[23] Note that $\hat{q}_\vartheta(\omega)$ is, generally speaking, not Hermitian, but $\hat{q}_\vartheta(\omega) = \hat{q}_\vartheta^\dagger(-\omega)$.

[24] The theory of Ref. [18] was developed for the case of zero one-photon detuning, i.e. symmetric EIT line. We used this approximation when constructing the fit.

[25] Neergard-Nielsen J S, Melholt-Nielsen B, Hettich C, Mølmer K and Polzik E S 2006 *Phys. Rev. Lett.* **97**, 083604

[26] Lvovsky A I 2004 *J. Opt. B: Quantum and Semiclassical Optics* **6** S556; Řeháček J, Hradil Z, Knill E and Lvovsky A I 2007 *Phys. Rev. A* **75**, 042108

[27] Phillips N B, Gorshkov A V and Novikova I 2008 *Phys. Rev. A* **78**, 023801